

## Electrochemical Impedance Spectroscopy Investigation of a Polyimide Coating on Q345 Steel

Yubao Qian<sup>1,2</sup>, Hongwu Zhu<sup>1</sup> and Ding Feng<sup>2,\*</sup>

<sup>1</sup> China University of Petroleum, Beijing, 102249, P.R. China

<sup>2</sup> Yangtze University, Jingzhou, 434023, P.R. China

\*E-mail: [fengd0861@163.com](mailto:fengd0861@163.com)

*Received:* 26 December 2016 / *Accepted:* 14 February 2017 / *Published:* 12 March 2017

---

In the present work, polyimide coated turbodrill Q345 steel was prepared with different coating thicknesses (30, 50 and 80  $\mu\text{m}$ ). The corrosion resistance properties of those samples (exposed to a 3.0% NaCl solution) were performed by electrochemical impedance spectroscopy (EIS). Obtained impedance parameters were utilized to evaluate the effectiveness of anticorrosive properties. Pull-off adhesion and microhardness of samples which was exposed before and after to the corrosive environment were carried out to reveal the relationships between the degradation process and the mechanical properties changes in coating/metal system. Polyimide coated samples exhibit high adhesion and enhanced anticorrosion characteristics.

---

**Keywords:** Electrochemical impedance spectroscopy; Corrosion; Polyimide; Pull-off adhesion; Microhardness

### 1. INTRODUCTION

Coiled tubing (CT) has gained a wide range of applications over the past decades. Accompanying with the development of drilling technology, CT has been extended to harsher conditions, such as at shallower depths, in more complex well profiles and more hostile environments. Therefore, it is of great importance to improve CT technology in order to perform effectively in those hostile environments, especially for workover and drilling operations, for instance grass roots drilling, sidetracking, and wellbore extensions [1-3]. However, up to date, CT technology is unable to achieve optimal performance in some cases, for example, the utilization of turbodrills. The application of turbodrills is beneficial to CT technology, although it has been eliminated from the use in CT in

history due to the corrosion of turbodrills during the drilling process [4-7]. Therefore, the enhancements of anti-corrosion properties of turbodrill greatly contribute to CT applications [8].

Organic coatings which can serve as a physical barrier to prevent the metal surface from corrosion in complex environments are useful for the protection of metals [9-12]. However, corrosive species like anions, metal ions, oxygen and water can permeate the polymer layers [13-17]. For example, water molecules presenting at the interface between metal and coating is harmful for the adhesion of coating to the metal surface, and thus results in a corrosion of metal. Therefore, the protection characteristics of the painted system mostly depend on the nature of the intermediate layers and metallic substrate [18-21]. In order to evaluate the anticorrosion properties of coated metals in corrosive environments, EIS (electrochemical impedance spectroscopy) as non-destructive analytic technique is available to be employed [22-25]. Relevant responses can be obtained by imposing a small amplitude alternating potential on the painted system. Thus, EIS spectra can supply useful information concerning to the corrosion properties.

Mac Diarmid [26], Wei [27], and their co-workers measured the corrosion protection performance of PANI. However, due to the poor solubility in common organic solvents, the practical application of PANI is limited in many fields. Electroactive polymers have also been synthesized through condensation polymerization process employing aniline oligomers for instance polyimide [28] and epoxy resin [29] as macro-monomers. However, the synthetic approaches of aniline oligomers involve multiple complex steps. Wei et al. and Zhang et al. have developed an oxidative coupling polymerization method for the coupling reaction of 1,4-phenylenediamine and oligoaniline [30-33]. The obtained polymers contain well-defined conjugated segments, and thus serve an opportunity to investigate conduction mechanism of conjugated polymers and relationships between structure and properties. But owing to the complex molecular structures and poor solubility in organic solvents, it is still difficult to fully understand the detailed mechanism and structure-property relationships. In addition, Wang et al. synthesized electroactive polymers containing an aniline oligomer in both main chain and side chain. As-obtained polymers shows high dielectric constants, good electrochemical properties and electrochromic behaviours [34].

In the present work, polyimide coatings were applied on Q345 steel, and the EIS, pull-off adhesion and microhardness were measured under the condition of exposure to an aerated electrolyte. Polyimide coating was employed because of its hardness and good adhesion to metals, and thus it provided a new polymer-based matrix to reveal the relationships between structure and electrochemical behaviour in the metal/coating system. Furthermore, the results of impedance, microhardness and pull-off adhesion were all obtained in order to investigate the influences of different adhesion extent between metallic substrates and organic coating on the corrosion resistance properties of these materials.

## 2. EXPERIMENTS

For synthesis of polyamide, 0.26 g 4,4'-oxydiphthalic anhydride (ODAD, 2 mmol) was firstly dissolved in NMP (10 mL), and then was introduced dropwise into an *N*-phenyl-*p*-phenylenediamine

solution (1.11 g, 6 mmol dissolved in NMP 10 mL) over 30 min followed by a magnetically stir process for 3 h. This solution was then poured into distilled water (100 mL) to obtain precipitation of electroactive oligoaniline. As-synthesized oligoaniline solid was filtered and then washed with dichloromethane and distilled water for several times. Subsequently, it was dried under room temperature and vacuum condition for 24 h. Finally, as-obtained oligoaniline powder was calcined at 260 °C for 5 h under dynamic vacuum condition for the oligoaniline imidization process. The yield of imidic form in oligoaniline was equal to ca. 90%. As-synthesized polyamide was firstly coated onto the surface of Q345 steel using drop-casting method followed by an air-dry process at 260 °C for at least 5 h in order to produce dense and uniform coatings with thickness of 30 to 80  $\mu\text{m}$ .

EIS spectra were measured by using a computer-controlled lock-in amplifier (EG&G Model 5210) connected with a potentiostat (EG&G Model 283A). Tests were carried out under cathodic polarisation conditions by imposing polarisation potentials that are equal to those typical sacrificial anodes (-1.0 V (SCE) with aluminium anodes and -1.5 V (SCE) with magnesium anodes [35]) Impedance results were studied under ambient temperature ( $\sim 20$  °C) condition by superimposing a voltage sine wave (15 mV (rms), 40 kHz–1 mHz) to the applied polarisation with 5 points per decade and more than four cycles at each frequency. *ZsimpWin* 2.00 software was then employed to acquire and analyse the obtained data in terms of Bode plots (logarithm of the impedance modulus  $|Z|$  and phase angle  $\Phi$  as a function of the logarithm of the frequency  $f$ ).

Direct pull-off adhesion measurements were used to perform pull-off adhesion of both initial adhesion and retained adhesion (immersed in a 0.5 M NaCl aqueous solution). An appropriate adhesive was used to bond the test dolly to the coating. For retained adhesion tests, samples were taken out of the NaCl solution after the immersion process, and then thoroughly washed with distilled water. Subsequently, they were dried at ambient temperature for 48 h. A digital adhesion tester (maximum load, 150 kg/cm) was employed.

The hardness of the coating was evaluated by using an ultrahardness tester with a knoop indenter (Anton Parr MHT-4), and the values of hardness were obtained by calculating the diagonal length of indentation.

### 3. RESULTS AND DISCUSSION

Impedance spectra of painted samples were collected with different exposure times (immersed in 3.0% NaCl solution), and results were showed in Fig. 1, Fig. 2 and Fig. 3. Both Bode (logarithm of the impedance magnitude and of the phase angle vs. the logarithm of the frequency) and Nyquist (imaginary component of impedance vs. the real component) plots were obtained. Results clearly suggest that electrochemical behaviour of polyimide coated samples greatly depends on the exposure time. The impedance diagram exhibiting a 90° phase shift over wide frequencies indicates that samples, especially coated with thick film, are highly capacitive in the first hours. A diffusion limiting current of oxygen reduction can be seen in the early stage of polarization. However, at lower potentials, the reduction of H<sub>2</sub>O becomes more dominant, leading to a progressive increase in the current density [36].

The two capacitive semicircles could be observed when thinner polyimide films-coated samples were exposure since the early times. In particular, the semicircles became most obvious when the coating was thinnest. A decrease of the impedance values of all the measured samples was observed in the diagrams of impedance during the first hour of the measurement.

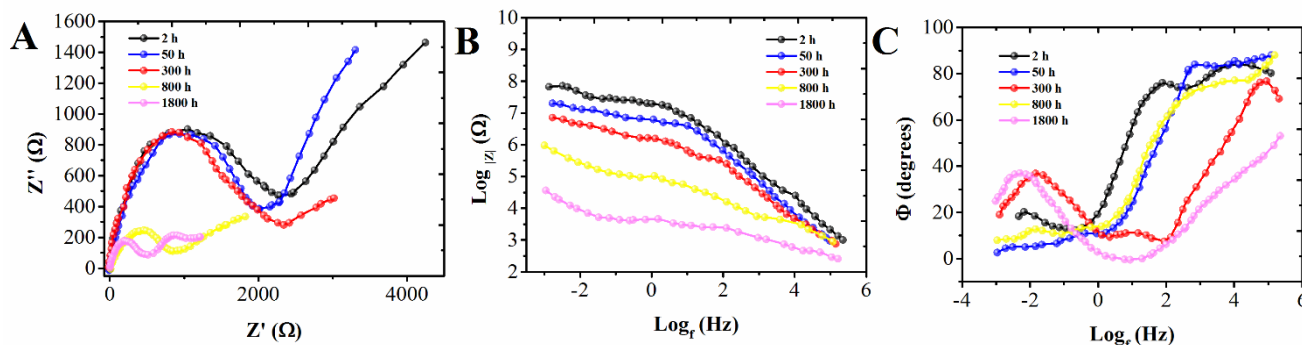


**Figure 1.** Experimental impedance diagrams of a Q345 steel covered by polyimide film with a thick of 60  $\mu\text{m}$  after being immersed for 2, 50, 300, 800, and 1800 h.

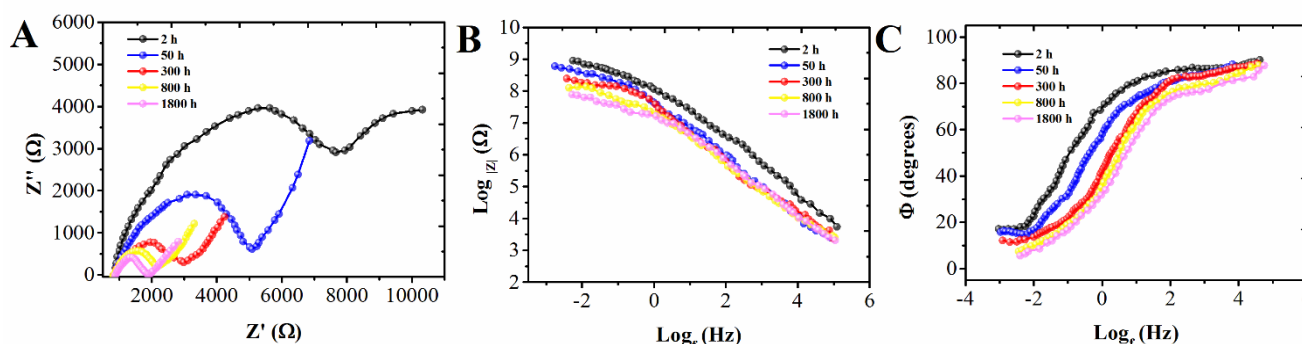


**Figure 2.** Experimental impedance diagrams of a Q345 steel covered by polyimide film with a thick of 80  $\mu\text{m}$  after being immersed for 2, 50, 300, 800, and 1800 h.

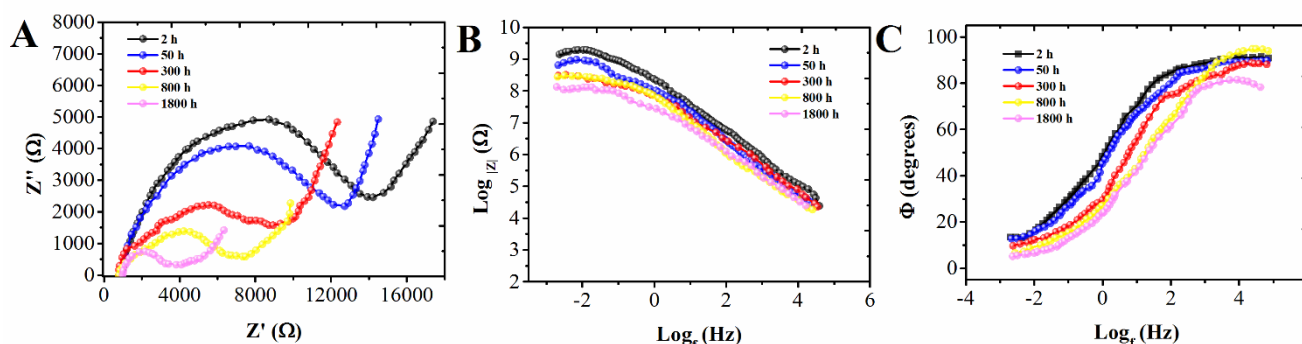


**Figure 3.** Experimental impedance diagrams of a Q345 steel covered by polyimide film with a thick of 100  $\mu\text{m}$  after being immersed for 2, 50, 300, 800, and 1800 h.

The original decay of the system impedance was significantly slow when the samples were covered by the coatings with a thick of 60 or 80  $\mu\text{m}$ , whereas the impedance increased after being exposed for 300 h. However, for the thinnest film, the impedance decreased all the time. The break-point approach designed by Haruyama et al. [37] was first employed to study the degradation of the coated specimens. For this approach, the values of the typical breakdown frequency  $f_b$ , which were in relation with the peeling region during the beginning of the peeling, were experimentally determined based on the impedance spectra. Specifically, the typical breakdown frequency  $f_b$  was the frequency between the capacitive-resistive transition range when the phase angle  $\theta$  was  $45^\circ$ .

Three different systems were employed to first investigate the pure capacity as well as characteristic of an efficient barrier film. The limit of the impedance modulus in the low frequency exhibited remarkably high value more than  $10^9 \Omega \text{ cm}^2$ , whereas the phase angle for most frequency range employed remained approximate to  $90^\circ$ . Whereas, this induces a charge transfer resistance ( $R_t$ ) increase which reveals an impeded charge transfer process, as a result of the shrinking of uncovered steel area [38]. According to the impedance spectra, it was obvious that only one-time constant could be obtained, which was attributed to the barrier characteristic of the organic coating. Figure 4A illustrated the simple equivalent circuit involving in a resistant constituent  $R_{PO}$  and a dielectric capacitor  $C_C$ , which was utilized to describe the electrochemical performance. The values of  $R_{PO}$ , which was beyond  $10^8 \Omega \text{ cm}^2$ , indicated that the polymeric film exhibited barrier characteristic. In particular, such values was high enough to efficiently isolate the metallic substrate the aggressive ambient. However, the frequency range became narrow with the elapsing time, indicated that the capacitive performance of the carbon steel covered with the coating was more remarkable based on the Bode phase diagrams. Meanwhile, the values of the impedance modulus decreased in the range of  $10^6$  to  $10^8 \Omega \text{ cm}^2$ . Hence, the remarkable frequency data suggested that the polymeric film exhibited an outstanding dielectric property.

The second-time constant from the impedance diagrams was developed after exposure for longer time, which could be observed from a second semicircle in the Nyquist diagrams at lower frequencies. During the degradation process of the coating, the sheltering effect of film partly lost in definite areas. The impedance increased since charge accumulation becomes progressively difficult as consequence of the ionic depletion. It can be stated that the bulk cannot be considered infinite and for very low frequencies the EIS results are progressively independent of the sample ionic content [39]. Hence, the underlying metal would directly contact with the aqueous ambient. Moreover, the sheltering feature of the integral organic film was illustrated through the first semicircle, where the erosion process at the interface of substrate and paint was explicated with the second semicircle, especially for the process of charge transfer between the metal and the solution. The equivalent circuit employed for the metal covered with defective organic coating under these conditions, which was illustrated in Figure 4B, explicated the measured impedance spectra sufficiently. For this model, a capacitor  $C_{DL}$  were employed as the new constituent, which clarified the ionic charge distribution surrounding the bare metallic substrate. Besides,  $R_t$  as a new resistant element was in inverse proportion with the corrosion rate of the metal.

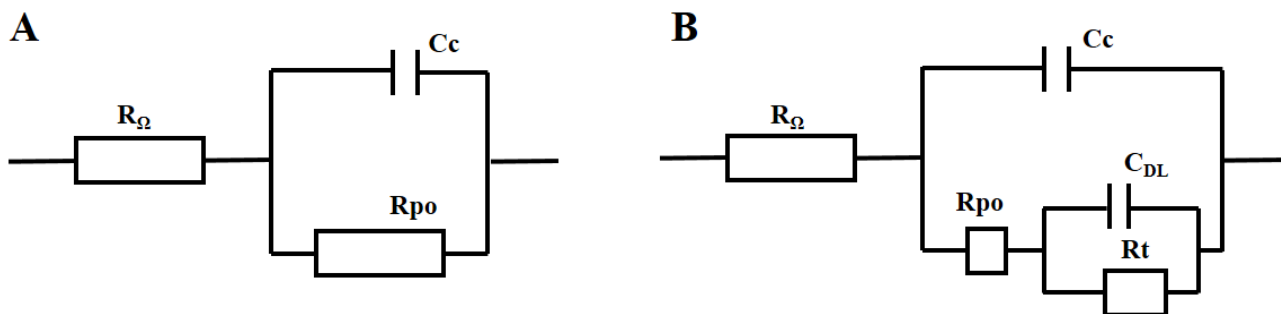


**Figure 4.** Equivalent circuits of (A) barrier-protected system with one time constant and (B) non-barrier-protected system with two time constants.

The polymeric film breakdown under exposure for longer time when the corrosion blisters developed, which would induce remarkably lower impedance among all the frequency range, according to the Bode-phase diagrams obtained through exposure for more than 1500 h. Therefore, the metal panels would not be protected from corrosion, resulting in the formation of blisters at the interface of metal and coating. For this case, the values of impedance were lower than  $10^6 \Omega \text{ cm}^2$ , where the breakdown frequencies were higher than  $10^2 \text{ Hz}$ . Figure 4 illustrated the equivalent circuits to analyse the impedance spectra, where the parameters  $R_{PO}$  and  $C_C$  were determined. Figure 5 explicated the plot of the magnitude changes of the parameters versus the time of exposure to the test solution for these three systems employed in this work. Besides, the capacity of the metal/coating systems was also studied through the values of the break-point frequency from the impedance spectra [40], which exhibited a phase angle ( $\phi$ ) of  $45^\circ$ . The breakdown frequency was a typical parameter in relation to the capacitive–resistive transition in the spectra, where the values were corresponded to the peeling region in the original stages of delamination based on the following equation [37, 41]:

$$f_b = \frac{A_d}{2\pi\xi\xi_0\rho_0A} = \frac{KA_d}{A}$$

In this equation,  $A_d$  represented the delaminated area and  $A$  depicted all the area of the sample. Besides, the vacuum capacity, the specific resistance coefficient of the coating in the peeling region and the permittivity of the organic coating were clarified through  $\varepsilon_0$ ,  $\varepsilon$  and  $\rho_0$ . Figure 5C illustrated the plot of the values of the breakpoint frequencies for the system taken in account against the exposure time. According to Díaz et al. [42], measurements made in immersed ionic material samples, such as cementitious ones, in which only a partial transversal area is exposed, are affected by the conducting occurring at the fringe of the samples. This phenomenon influences the resistance values of the analysed samples, causing apparent resistivity values lower than the real ones.

The pull-off tests were carried out to study the adhesive force of the organic coatings towards the metallic substrates, where adhesion was quantified through the forces utilized to detach the paint film glued with the test dollies from the underlying metal. The samples before exposure as well as after electrochemical tests were studied. Table 1 showed the adhesion values measured through the pull-off tests. The forces required to detach the film from the specimens after exposure to the electrolyte solution were lower than those of the specimens without exposure. In particular, such decrease was

rather significant for the galvanized steel panels covered with organic coatings, whereas it was remarkably low for the Q345 steel-painted samples.

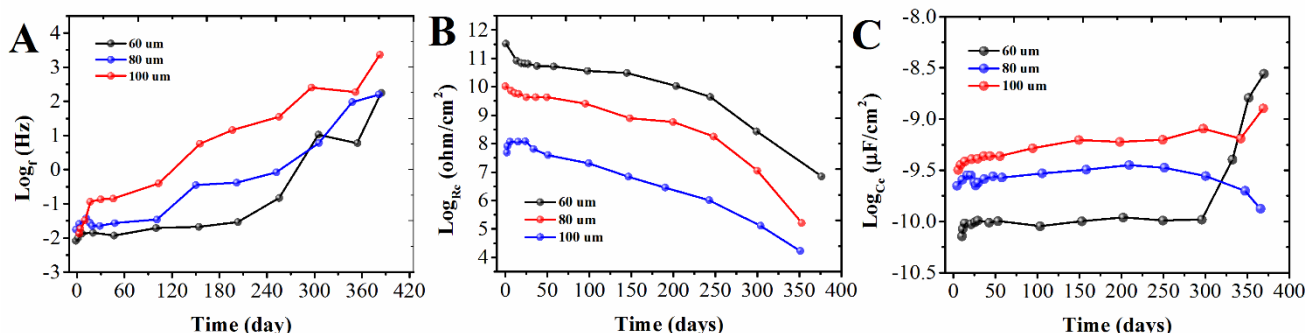


**Figure 5.** Time course of the impedance parameters: (A) coating capacitance  $C_C$ , (B) pore resistance  $R_{PO}$  and (C) breakdown frequency  $f_b$ .

**Table 1.** Pull-off test results.

Sample characteristic	No exposure	After exposure
30 µm thick coating	63.4	61.8
50 µm thick coating	29.7	28.4
80 µm thick coating	26.1	22.4

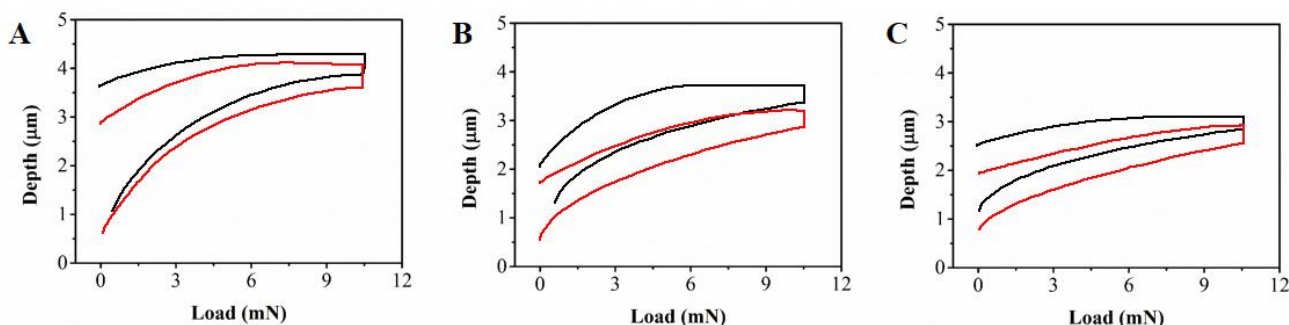


**Figure 6.** Hardness vs load of these three metal/coating systems before and after exposure to NaCl solution with a concentration of 0.5 M for three month. (A) Q345 steel coated by polyimide film with a thick of 60 µm ; (B) Q345 steel coated by polyimide film with a thick of 80 µm; and (C) Q345 steel coated by polyimide film with a thick of 100 µm.

Mechanical parameters of the coated specimens including the plastic composition ( $HU_{pl}$ ), Martens microhardness (HM) and the indentation modulus (EIT) before and after performing the electrochemical measurements were investigated. Figure 6 depicted the loading/unloading curves of the depth of indentation versus the load for the polyimide coating deposited on the Q345 steel with various thickness. The curve was based on the average of 5 measurements carried out at 5 different

points on the material surface. The mechanical performance of the films in all the cases was approximate to that of the plastic material. Besides, the maximum loading was chosen to be 10 mN, as higher loads could induce the change of the slope of the relevant plots, where the whole tested hardness of the specimens were influenced by the metallic substrate.

#### 4. CONCLUSIONS

In conclusion, the electrochemical performance of the polyimide coating, which was deposited directly on the turbodrill Q345 steel, could be evaluated through the time course of the impedance parameters obtained by application of the as-formed equivalent circuit. The results indicated the polyimide film exhibited a less efficient protection for the underlying metal. The capacitance of the coating increased, whereas the resistance of the coating decreased. Furthermore, the protection for the metallic system was enhanced when depositing thicker polyimide film on the turbodrill Q345.

#### ACKNOWLEDGEMENT

This work has been supported by the National Natural Science Foundation of China (Grant No. 51275057)

#### References

1. Y.A. Shirinkin and E. Teploukhov, *Chemical and Petroleum Engineering*, 27 (1991) 367.
2. Y.V. Sadykhov, B. Es' man, R.S. Azizbekov, E. Zhidkov and V. Dymov, *Chemical and Petroleum Engineering*, 27 (1991) 368.
3. M. Yaroshenko, L. Mirzoyan and S. Kaufman, *Chemical and Petroleum Engineering*, 28 (1992) 131.
4. Y.V. Lakhotkin, V. Dushik, V. Kuz'min and N. Rozhanskii, *Protection of Metals and Physical Chemistry of Surfaces*, 51 (2015) 1165.
5. E. Medvedovski, *Ceram. Int.*, 39 (2013) 2723.
6. I. Smurov, M. Doubenskaia, S. Grigoriev, D. Kotoban and P. Podrabinnik, *Journal of Friction and Wear*, 35 (2014) 470.
7. T. Ma, P. Chen and J. Zhao, *Geomechanics and Geophysics for Geo-Energy and Geo-Resources*, 2 (2016) 365.
8. V.B. Batalovic, *Proceedings of the Institution of Mechanical Engineers, Part E: Journal of Process Mechanical Engineering*, 226 (2012) 263.
9. Z. Zhou, M. Wang, L. Liu and Z. Wang, *Ceramics–Silikáty*, 60 (2016) 254.
10. D. Xia, S. Song, J. Wang, H. Bi and Z. Han, *Transactions of Tianjin University*, 18 (2012) 15.
11. A.W. Momber, S. Buchbach, P. Plagemann and T. Marquardt, *Progress in Organic Coatings*, 101 (2016) 186.
12. M. Deyab and S. Keera, *Mater. Chem. Phys.*, 146 (2014) 406.
13. M. Zheludkevich, J. Tedim and M. Ferreira, *Electrochimica Acta*, 82 (2012) 314.
14. A. Stankiewicz, I. Szczygieł and B. Szczygieł, *Journal of Materials Science*, 48 (2013) 8041.
15. P. Rodič, J. Iskra and I. Milošev, *Journal of sol-gel science and technology*, 70 (2014) 90.
16. D. Balgude and A. Sabnis, *Journal of sol-gel science and technology*, 64 (2012) 124.
17. J. Wang, S. Song, K. Wang, C. Shen, B. Luo and J. Shi, *Journal of Wuhan University of*

- Technology-Mater. Sci. Ed.*, 28 (2013) 367.
18. V. Barranco, A. Jiménez-Morales, E. Peón, G. Hickman, C. Perry and J. Galván, *Journal of Materials Chemistry B*, 2 (2014) 3886.
  19. K. Chang, C. Hsu, H. Lu, W. Ji, C. Chang, W. Li, T. Chuang, J. Yeh, W. Liu and M. Tsai, *Express Polym. Lett*, 8 (2014) 243.
  20. D. Enning and J. Garrelfs, *Applied and environmental microbiology*, 80 (2014) 1226.
  21. J. Li, J. Cui, J. Yang, Y. Ma, H. Qiu and J. Yang, *Progress in Organic Coatings*, 99 (2016) 443.
  22. S.B. Aoun, M. Bouklah, K. Khaled and B. Hammouti, *Int. J. Electrochem. Sci*, 11 (2016) 7343.
  23. D. Mareci, I. Rusu, R. Chelariu, G. Bolat, C. Munteanu, D. Sutiman and R. Souto, *European Journal of Science and Theology*, 9 (2013) 189.
  24. Y. Zhang, Y. Shao, G. Meng, T. Zhang, P. Li and F. Wang, *Journal of Coatings Technology and Research*, 12 (2015) 777.
  25. C. Yu, P. Wang, X. Gao and H. Wang, *Int. J. Electrochem. Sci*, 10 (2015) 538.
  26. N. Ahmad and A.G. MacDiarmid, *Synthetic Metals*, 78 (1996) 103.
  27. Y. Wei, J. Wang, X. Jia, J.-M. Yeh and P. Spellane, *Polymer*, 36 (1995) 4535.
  28. K.-Y. Huang, Y.-S. Jhuo, P.-S. Wu, C.-H. Lin, Y.-H. Yu and J.-M. Yeh, *European Polymer Journal*, 45 (2009) 485.
  29. K.-Y. Huang, C.-L. Shiu, P.-S. Wu, Y. Wei, J.-M. Yeh and W.-T. Li, *Electrochimica Acta*, 54 (2009) 5400.
  30. D. Chao, X. Ma, Q. Liu, X. Lu, J. Chen, L. Wang, W. Zhang and Y. Wei, *European polymer journal*, 42 (2006) 3078.
  31. D. Chao, L. Cui, X. Lu, H. Mao, W. Zhang and Y. Wei, *European polymer journal*, 43 (2007) 2641.
  32. D. Chao, X. Lu, J. Chen, X. Liu, W. Zhang and Y. Wei, *Polymer*, 47 (2006) 2643.
  33. D. Chao, X. Ma, X. Lu, L. Cui, H. Mao, W. Zhang and Y. Wei, *Journal of applied polymer science*, 104 (2007) 1603.
  34. D. Chao, J. Zhang, X. Liu, X. Lu, C. Wang, W. Zhang and Y. Wei, *Polymer*, 51 (2010) 4518.
  35. R. Souto and D. Scantlebury, *Progress in organic coatings*, 53 (2005) 63.
  36. A.P. Yadav, A. Nishikata and T. Tsuru, *Corrosion Science*, 46 (2004) 169.
  37. R. Hirayama and S. Haruyama, *Corrosion*, 47 (1991) 952.
  38. J. Marin-Cruz, R. Cabrera-Sierra, M. Pech-Canul and I. Gonzalez, *Electrochimica Acta*, 51 (2006) 1847.
  39. A.S. Castela, B.S. da Fonseca, R.G. Duarte, R. Neves and M.F. Montemor, *Electrochimica Acta*, 124 (2014) 52.
  40. N.J. Kouloumbi and S.T. Kyvelidis, *Microchim. Acta.*, 136 (2001) 175.
  41. J.N. Murray, *Progress in Organic Coatings*, 30 (1997) 225.
  42. B. Diaz, L. Freire, X.R. Novoa, B. Puga and V. Vivier, *Cement & Concrete Research*, 40 (2010) 1465.